7448 *Biochemistry* **2009,** *48,* 7448–7456
DOI: 10.1021/bi9004914

BIOCHEMISTRY
including biophysical chemistry & molecular biology
Article

Functional Importance of GGXG Sequence Motifs in Putative Reentrant Loops of 2HCT and ESS Transport Proteins†

Adam Dobrowolski and Juke S. Lolkema*

Molecular Microbiology, Groningen Biomolecular Sciences and Biotechnology Institute, University of Groningen, Haren, The Netherlands

Received March 23, 2009; Revised Manuscript Received July 10, 2009

ABSTRACT: The 2HCT and ESS families are two families of secondary transporters. Members of the two families are unrelated in amino acid sequence but share similar hydropathy profiles, which suggest a similar folding of the proteins in membranes. Structural models show two homologous domains containing five transmembrane segments (TMSs) each, with a reentrant or pore loop between the fourth and fifth TMSs in each domain. Here we show that GGXG sequence motifs present in the putative reentrant loops are important for the activity of the transporters. Mutation of the conserved Gly residues to Cys in the motifs of the Na^+-citrate transporter CitS in the 2HCT family and the Na^+-glutamate transporter GltS in the ESS family resulted in strongly reduced transport activity. Similarly, mutation of the variable residue "X" to Cys in the N-terminal half of GltS essentially inactivated the transporter. The corresponding mutations in the N- and C-terminal halves of CitS reduced transport activity to 60 and 25% of that of the wild type, respectively. Residual activity of any of the mutants could be further reduced by treatment with the membrane permeable thiol reagent *N*-ethylmaleimide (NEM). The X to Cys mutation (S405C) in the cytoplasmic loop in the C-terminal half of CitS rendered the protein sensitive to the bulky, membrane impermeable thiol reagent 4-acetamido-4′-maleimidylstilbene-2,2′-disulfonic acid (AmdiS) added at the periplasmic side of the membrane, providing further evidence that this part of the loop is positioned between the transmembrane segments. The putative reentrant loop in the C-terminal half of the ESS family does not contain the GGXG motif, but a conserved stretch rich in Gly residues. Cysteine-scanning mutagenesis of a stretch of 18 residues in the GltS protein revealed two residues important for function. Mutant N356C was completely inactivated by treatment with NEM, and mutant P351C appeared to be the counterpart of mutant S405C of CitS; the mutant was inactivated by AmdiS added at the periplasmic side of the membrane. The data support, in general, the structural and mechanistic similarity between the ESS and 2HCT transporters and, more particularly, the two-domain structure of the transporters and the presence and functional importance of the reentrant loops present in each domain. It is proposed that the GGXG motifs are at the vertex of the reentrant loops.

The 2HCT [2-hydroxycarboxylate transporter, TC 2.A.24 (*1*)] and ESS (glutamate:Na^+ symporter, TC 2.A.27) families represent families of ion-driven transporter proteins that are exclusively found in the bacterial domain. Members of the two families do not share any significant amino acid sequence similarity, but the hydropathy profiles of the sequences are very similar. For this reason, the two families are in the same structural class (ST[3]) in the MemGen classification system that we have introduced to identify membrane proteins sharing the same fold (*2*−*5*). The MemGen classification system groups membrane proteins in structural classes based on hydropathy profile analysis. The hydropathy profile of the amino acid sequence of the membrane protein is taken to be characteristic for the folding of the protein in the membrane. Recently, strong support for the MemGen classification was obtained by the similar organization of the core in the high-resolution structures of members of the NSS [neurotransmitter sodium symporter, TC 2A.22 (*6*)], SSS [sodium solute symporter, TC 2A.21 (*7*)], and NCS1 [nucleobase cation symport 1, TC 2A.39 (*8*)] transporter families. While the members of the NSS, SSS, and NCS1 families do not share sequence similarity, the families are all found in the same structural class (ST[2]) in the MemGen classification (*3*, *9*).

Experimental support for the same fold of the proteins in the 2HCT and ESS families was obtained by demonstrating a similar membrane topology for two transporters from the two families (*10*). The well-established membrane topology model of the 2HCT family, mostly based on studies of Na^+-citrate transporter CitS of *Klebsiella pneumoniae* (reviewed in ref *11*), was used to predict the membrane topology of Na^+-glutamate transporter GltS of *Escherichia coli* (*12*, *13*), a member of the ESS family. The model was verified by accessibility studies of cysteine residues introduced into the GltS protein (*10*). Though membrane topology of a protein represents a low structural resolution, the result is not trivial and does validate the MemGen classification because of specific structural features of these proteins. Secondary structure predictors like TMHMM (*14*) predict different models for both CitS and GltS that were inconsistent with the experimental data (*10*).

The structural model of the transporters in the ESS and 2HCT families, and in all 33 families of structural class ST[3] in the

†This work was supported by grants from The Netherlands Organization for Scientific Research (NWO-ALW).

*To whom correspondence should be addressed: Molecular Microbiology, Biological Centre, Kerklaan 30, 9751 NN Haren, The Netherlands. Phone: +31 50 363 2155. Fax: +31 50 363 2154. E-mail: j.s.lolkema@rug.nl.

 Published on Web 07/13/2009

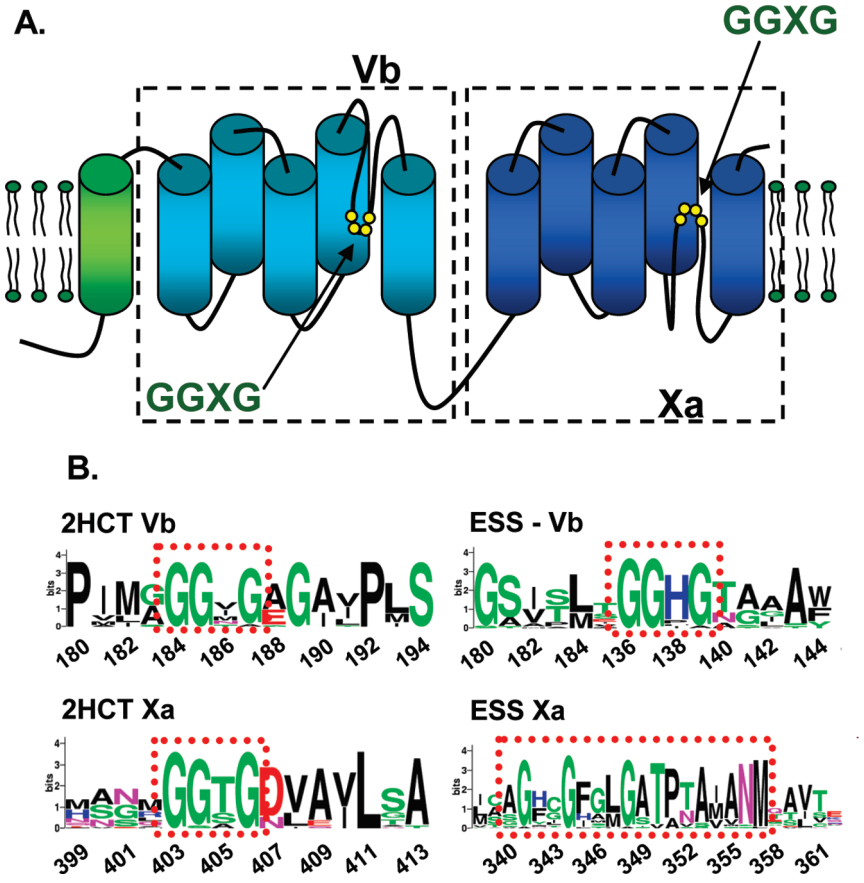

FIGURE 1: (A) Structural model for the transporters of the 2HCT and ESS families. Two homologous domains containing five TMSs each with an inverted topology in the membrane are indicated in dashed boxes. Each domain contains a pore loop structure entering the membrane-embedded part of the protein from the periplasmic and cytoplasmic sides of the membrane, respectively (Vb and Xa). Members of the 2HCT family have an additional TMS at the N-terminus that is not present in members of the ESS family. (B) Sequence logos of regions Vb and Xa showing the GGXG sequence motifs in the 2HCT (left) and ESS (right) families. Position numbers correspond to the residue numbers in the CitS (2HCT) and GltS (ESS) sequences. Residues mutated into cysteines are indicated in the red dotted boxes. The logos were generated using WebLogo, version 2.8.1 (http://www.bio.cam.ac.uk/cgi-bin/seqlogo/logo.cgi).

MemGen classification, consists of two domains each containing five transmembrane segments (Figure 1A). The total number of transmembrane segments is variable between different families. For instance, the 2HCT proteins have an additional segment at the N-terminus which is missing in the ESS proteins. In the model, the two domains of five TMSs each share a similar fold but have opposite orientations in the membrane (*11*, *15*, *16*), a structural motif seen more frequently in membrane proteins (inverted topology) (*6*−*8*, *17*−*20*). The loops between the fourth and fifth transmembrane segments in each domain are believed to form so-called pore loops or reentrant loops, which fold back between the transmembrane segments from opposite sides of the membrane [trans-reentrant loops (*15*, *16*)]. The reentrant loops in the N- and C-terminal domains are believed to be in close vicinity in the three-dimensional structure and to form the translocation pathway for substrate and co-ions.

The putative reentrant loop regions, termed Vb in the N-terminal domain and Xa in the C-terminal domain, are well conserved within the families throughout structural class ST[3] and contain a remarkably high fraction of residues with small side chains like Gly, Ala, and Ser (*11*). In almost all families of ST[3], small stretches of highly conserved residues are found in putative reentrant loop regions Vb and Xa. Sequence analysis of the 138 members of the ESS family and the 74 members of the 2HCT family showed that in the Vb regions of both families and the Xa region of the 2HCT family these conserved stretches contain a GGXG sequence motif in which X is a less conserved residue (see Figure 1B). The same motif cannot be found in the Xa region of the ESS family, but also here, three conserved Gly residues are found in a stretch of eight residues.

Here, we present a mutational study of the GGXG sequence motifs found in the putative reentrant loops of the CitS and GltS proteins in determining the relevance of the motifs for the transport function of the proteins. The functional relevance of the Xa region in GltS in which the motif is not found is addressed by cysteine-scanning mutagenesis. It follows that the motifs play an important role in the transport mechanism catalyzed by both transporters, and further evidence for the existence of the reentrant loops is obtained. The corresponding properties of CitS and GltS further support a similar core structure and mechanism for the two transport proteins.

EXPERIMENTAL PROCEDURES

Bacterial Strains, Growth Conditions, and GltS and CitS Constructs. *E. coli* strain DH5α was routinely grown in Luria-Bertani broth (LB) medium at 37 °C while being continuously shaken at 150 rpm. Ampicillin was used at a final concentration of 50 μg/mL. The GltS and CitS proteins were expressed in *E. coli* DH5α cells harboring plasmid pBAD24 (Invitrogen) derivatives encoding the wild type or cysteine mutants of GltS (*10*) and CitS (*23*) extended with six additional histidine residues at the N-terminus (His tag). In the case of CitS variants, a sequence

encoding an enterokinase cleavage site was present between the His tag and the *citS* gene. Expression of genes cloned in pBAD24 is under the control of the arabinose promoter. Production of the GltS and CitS proteins was induced by addition of 0.01% arabinose when the optical density of the culture measured at 660 nm (OD_{660}) reached a value of 0.6. The cysteine mutants of GltS and CitS were constructed by PCR using the QuickChange site-directed mutagenesis kit (Stratgene, La Jolla, CA). All mutants were sequenced to confirm the presence of the desired mutations (ServiceXS, Leiden, The Netherlands).

Transport Assays in RSO Membranes. *E. coli* DH5α cells expressing CitS or GltS variants were harvested from a 1 L culture by centrifugation at 10000*g* for 10 min at 4 °C. Right-side-out (RSO) membrane vesicles were prepared by the osmotic lysis procedure as described previously (*21*). RSO membranes were resuspended in 50 mM KP_i (pH 7), rapidly frozen, and stored in liquid nitrogen. The membrane protein concentration was determined by the DC protein assay kit (Bio-Rad Laboratories, Hercules, CA).

Uptake by RSO membranes was assessed by the rapid filtration method. The membranes were energized using the potassium ascorbate/phenazine methosulfate (PMS) electron donor system (*22*). Membranes were diluted to a final concentration of 0.5 mg/mL in 50 mM KP_i (pH 6.0) containing 70 mM Na^+, in a total volume of 100 μL at 30 °C. Under a constant flow of water-saturated air, and while the mixture was being stirred magnetically, 10 mM potassium ascorbate and 100 μM PMS (final concentrations) were added, and the proton motive force was allowed to develop for 2 min. Then, L-[^{14}C]glutamate or [1,5-^{14}C]citrate was added at a final concentration of 1.9 or 4.4 μM, respectively. Uptake was stopped by the addition of 2 mL of ice-cold 0.1 M LiCl, followed by immediate filtration over cellulose nitrate filters (0.45 μm, pore size). The filters were washed once with 2 mL of a 0.1 M LiCl solution and assayed for radioactivity. The background was estimated by adding the radiolabeled substrate to the vesicle suspension after the addition of 2 mL of ice-cold LiCl, immediately followed by filtering.

Partial Purification of GltS and CitS Derivatives by Ni^{2+}-NTA Affinity Chromatography. *E. coli* DH5α cells expressing CitS or GltS variants were harvested from a 200 mL culture by centrifugation at 10000*g* for 10 min at 4 °C. Cells were washed with 50 mM KP_i buffer (pH 7) and resuspended in 2 mL of the same buffer and, subsequently, broken with a Soniprep 150 sonicator operated at an amplitude of 8 μm by nine cycles consisting of 15 s ON and 45 s OFF. Cell debris and unbroken cells were removed by centrifugation at 9000 rpm for 5 min. Membranes were collected by ultracentrifugation for 25 min at 80000 rpm and 4 °C in a Beckman TLA 100.4 rotor and washed once with 50 mM KP_i (pH 7.0).

His-tagged GltS and CitS derivatives were partially purified from the cytoplasmic membranes or RSO membranes prepared as described above using Ni^{2+}-NTA affinity chromatography as follows. Membranes (4 mg/mL) were solubilized in 50 mM KP_i (pH 8), 400 mM NaCl, 20% glycerol, and 1% Triton X-100 followed by incubation for 30 min at 4 °C under continuous shaking. Undissolved material was removed by ultracentrifugation at 80000 rpm for 25 min at 4 °C. The supernatant was mixed with Ni^{2+}-NTA resin (50 μL bed volume per 5 mg of protein), equilibrated in 50 mM potassium phosphate (pH 8.0), 600 mM NaCl, 10% glycerol, 0.1% Triton X-100, and 10 mM imidazole, and incubated overnight at 4 °C under continuous shaking. Subsequently, the column material was pelleted by pulse centrifugation, and the supernatant was removed. The resin was washed with 10 volumes of equilibration buffer containing 300 mM NaCl and 40 mM imidazole. The protein was eluted with one-half of a bed volume of the washing buffer but containing 150 mM imidazole. The eluted fraction was stored at −20 °C until it was used.

Treatment of RSO Membrane Vesicles with Thiol Reagents. Stock solutions of the thiol reagents *N*-ethylmaleimide (NEM) and 4-acetamido-4′-maleimidylstilbene-2,2′-disulfonic acid (AmdiS) were prepared freshly in water. The treatment of the reagents was stopped by addition of an equal concentration of dithiothreitol (DTT). The presence of DTT did not affect the initial rate of uptake in transport assays. RSO membranes at a concentration of 1 mg/mL were treated for the indicated times and at the indicated temperatures with the thiol reagents in 50 mM KP_i (pH 7.0). Following treatment, RSO membranes were diluted twice into 50 mM KP_i (pH 5.0) containing 140 mM NaCl. The pH of the resulting suspension was 6.0, and the suspension was immediately used for uptake measurements.

Materials. NEM was purchased from Sigma-Aldrich BV (Zwijndrecht, The Netherlands), and AmdiS was purchased from Molecular Probes Europe BV (Leiden, The Netherlands). L-[^{14}C]Glutamate and [1,5-^{14}C]citrate were obtained from Amersham Pharmacia (Roosendaal, The Netherlands).

RESULTS

GGNG Sequence Motif in Region Vb of CitS. Each of the amino acid residues in sequence motif 184-GGNG-187 found in the Vb region of the Na^+-citrate transporter CitS of *K. pneumoniae* in the 2HCT family was substituted with a cysteine residue. The four mutants, G184C, G185C, N186C, and G187C, were tested for their ability to accumulate [1,5-^{14}C]citrate in right-side-out (RSO) membrane vesicles prepared from *E. coli* DH5α cells expressing the mutants. Citrate uptake was assessed in the presence of a proton motive force (pmf) that was generated using the artificial potassium ascorbate/PMS electron donor system (Figure 2A). RSO membrane vesicles prepared from cells not expressing CitS lack citrate uptake activity because of the absence of a citrate transport system in the *E. coli* membrane. Membranes containing mutants G184C and G187C exhibited a similar uptake activity that was ~10−15% of the activity of membranes containing wild-type CitS, while the G185C mutation resulted in complete lack of activity (Figure 2A). Mutation of the nonconserved position in the motif, N186 to Cys, resulted in an uptake activity of approximately 75% of that of wild-type CitS. Protein levels of the mutants in the membranes were estimated by small-scale purifications making use of the N-terminally fused His tag and Ni-NTA affinity chromatography (Figure 2B). All mutants exhibited similar expression levels as observed for wild-type CitS, indicating that the lower transport activity of the membranes containing the mutants was a consequence of the mutation in CitS rather than the lack of production or degradation of the proteins. It follows that the conserved Gly residues in the GGXG motif at positions 184 and 187 and especially Gly185 appear to be critical for the activity of the protein while mutation of the nonconserved N186 to Cys had an only marginal effect on the specific activity of CitS.

N-Ethylmaleimide (NEM) is a small, membrane permeable thiol reagent. Treatment of the RSO membrane vesicles containing wild-type CitS, which contains five cysteine residues, with 1 mM NEM results in a slow inactivation of the protein to 10−20% of wild-type activity with a half-time of inactivation

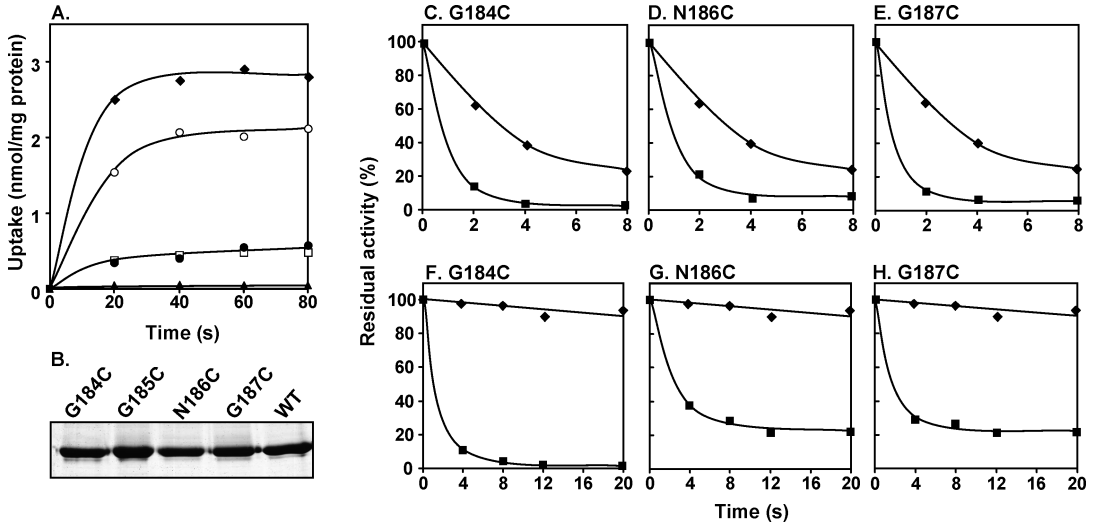

FIGURE 2: GGNG sequence motif in Vb of CitS of *K. pneumoniae*. (A) [1,5-^{14}C]citrate uptake in RSO membrane vesicles containing CitS (◆) and CitS mutants G184C (●), G185C (▲), N186C (○), and G187C (□). (B) SDS-PAGE of partially purified CitS and the G184C, G185C, N186C, and G187C mutants purified from the RSO membranes used in the uptake assays shown in panel A. (C−H) Residual activity after treatment of RSO membranes containing CitS (◆) and the mutants (■) G184C (C and F), N186C (D and G), and G187C (E and H) with 1 mM NEM (C−E) or 0.25 mM AmdiS (F−H) for the indicated time. Initial rates were expressed as the percentage of the initial rate catalyzed by untreated membranes.

of ~4 min (*23*) (Figure 2C−E). In contrast, the three mutations in the GGxG motif that resulted in CitS proteins with residual activity (G184C, N186C, and G187C) rendered the proteins highly sensitive to NEM with inactivation half-times of < 1 min. Moreover, treatment with NEM resulted in a lack of significant residual activity (Figure 2C−E).

The site of reaction of wild-type CitS with NEM consists of two cysteine residues in cytoplasmic region Xa (*23*). Consequently, wild-type CitS is not inactivated by AmdiS, a maleimide derivative containing a bulky, negatively charged group that, in contrast to NEM, is membrane impermeable and cannot reach these sites (Figure 2F−H). In contrast, the three active cysteine mutants in the GGNG motif, G184C, N186C, and G187C, were rapidly inactivated by AmdiS, with half-times ranging from 1 to 3 min, demonstrating that the introduced cysteine residues were readily accessible from the periplasmic side of the membrane (Figure 2F−H). Residual activity of the membranes containing mutants N186C and G187C was around 20% after treatment with AmdiS, while membranes containing mutant G184C no longer exhibited significant activity.

Mutants G184C, N186C, and G187C were constructed in a Cys-less version of CitS (*24*) to reveal the site of reaction of the mutants with the thiol reagents. Unfortunately, uptake activity by these mutants in RSO membrane vesicles was to low to measure transport in a reliable way. The low activity correlated with a low level of the CitS protein in the membrane (not shown). As an alternative, corresponding mutants with Ala replacements were constructed in the wild-type background. Mutants G184A and N186A exhibited the same residual activity after treatment with NEM as observed for the wild type, while both mutants were insensitive to treatment with AmdiS, strongly indicating that in the G184C and N186C mutants, the introduced Cys residues were modified by the thiol reagents (Table 1). Similarly, mutant G187A was insensitive to AmdiS, showing that the Cys residue at position 187 in the G187C mutant was modified by AmdiS and responsible for the inactivation of the transporter. Remarkably, inactivation of the G187A mutant by NEM was the same as observed for the G187C mutant, suggesting that the Gly to Ala mutation increased the reactivity of the endogenous Cys residues with NEM. In this respect, the G187A mutant in the Vb region of CitS behaves like the C398S mutant described previously (*23*). Cys398 is situated in the Xa region of CitS.

Table 1: Residual Activity after Treatment of RSO Membrane Vesicles Containing Wild-Type (WT) CitS and Cysteine (Cys) and Alanine (Ala) Mutants with NEM and AmdiS[a]

		residual activity[b] (%)	
position	inhibitor	Cys	Ala
G184	NEM	12 ± 3	62 ± 6
	AmdiS	2 ± 3	95 ± 5
N186	NEM	21 ± 4	55 ± 4
	AmdiS	22 ± 6	95 ± 2
G187	NEM	11 ± 3	5 ± 8
	AmdiS	21 ± 4	99 ± 5
S405	NEM	42 ± 5	68 ± 5
	AmdiS	5 ± 5	97 ± 3
WT	NEM	63 ± 6	
	AmdiS	96 ± 3	

[a] RSO membranes were treated with 1 mM NEM for 2 min and 0.25 mM AmdiS for 12 min. [b] The indicated values give the residual uptake activity in RSO membranes as the percentage of an untreated sample. The average and standard deviation of two or three independent measurements are reported.

GGHG Sequence Motif in Region Vb of GltS. In Na^+-glutamate transporter GltS of *E. coli*, the GGXG motif in the periplasmic Vb region is represented by residues 136-GGHG-139. In a similar approach as a described for CitS above, each position was mutated to a Cys residue and activities of the mutants were evaluated in RSO membranes. Membrane vesicles prepared from *E. coli* DH5α cells contain a basal level of glutamate transport activity due to endogenous glutamate transporters encoded on the chromosome (*25*). The background activity was estimated in membrane vesicles containing citrate transporter CitS produced from the same expression system (Figure 3A). CitS does not transport L-glutamate. RSO membranes containing plasmid-encoded GltS showed an activity that was approximately 5 times higher than the background activity

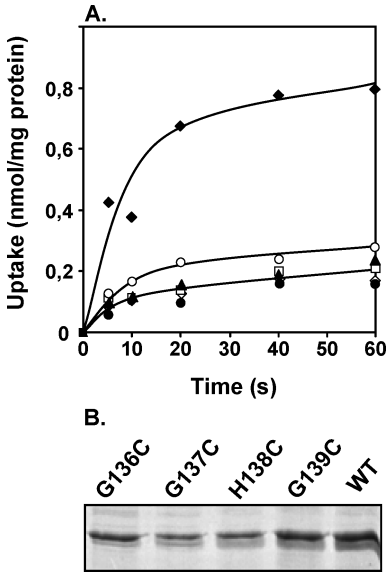

FIGURE 3: GGHG sequence motif in Vb of GltS of *E. coli*. (A) L-[^{14}C]Glutamate uptake in RSO membrane vesicles containing GltS (◆) and GltS mutants G136C (□), G137C (▲), H138C (●), and G139C (○), and CitS as a control (▼). (B) SDS−PAGE of partially purified GltS and mutants G136C, G137C, H138C, and G139C purified from the RSO membranes used in the uptake assays shown in panel A.

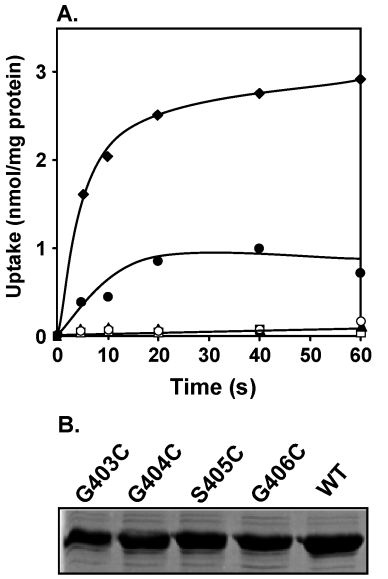

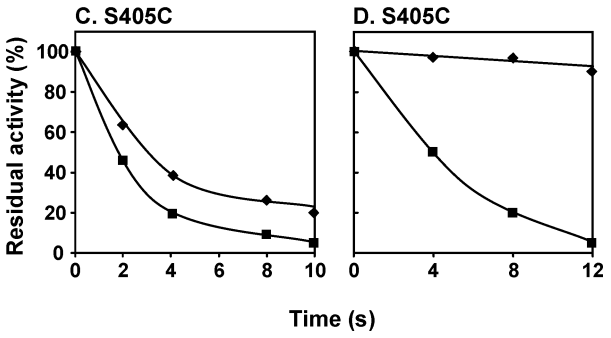

FIGURE 4: GGSG sequence motif in region Xa of CitS of *K. pneumoniae*. (A) [1,5-^{14}C]citrate uptake in RSO membrane vesicles containing CitS (◆) and the CitS mutants G403C (□), G404C (▲), S405C (●), and G406C (○). (B) SDS−PAGE of partially purified CitS and mutants G403C, G404C, S405C, and G406C purified from the RSO membranes used in the uptake assays shown in panel A. (C and D) Residual activity after treatment of CitS (◆) and the mutant G405C (■) with 1 mM NEM (C) or 0.25 mM AmdiS (D) for the indicated time. Initial rates were expressed as the percentage of the initial rate catalyzed by untreated membranes.

(Figure 3A). RSO membrane vesicles containing GltS mutants G136C, G137C, and H138C showed an uptake activity similar to the background level (Figure 3A). Mutant G139C repeatedly revealed an activity slightly above background, but potential changes in the background activity do not allow for a firm conclusion about the significance of this residual activity. Partial purification of the proteins showed that the lack of activity was not due to a lack of production of the proteins (Figure 3B). It follows that mutations in the sequence motif in region Vb of GltS are deleterious for the transport activity of the protein.

GGSG Sequence Motif in Region Xa of CitS. The GGXG sequence motif in cytoplasmic region Xa of CitS is represented by residues 403-GGSG-406. As observed for the motif in the Vb region of CitS, the least conserved residue in the motive was the least sensitive to mutation to a Cys residue. Membranes containing mutant S405C showed a relative uptake activity of approximately 40% of that of wild-type CitS, while mutation of the three Gly residues to Cys (G403C, G404C, and G406C) resulted in membranes with no significant citrate uptake activity (Figure 4A). Expression levels of the mutants were not significantly different from the wild-type level (Figure 4B).

Evidence of the folding of the cytoplasmic Xa region between the transmembrane segments as a reentrant loop structure followed from the accessibility of two endogenous Cys residues, Cys398 and Cys414, for the small, charged thiol reagent 2-(trimethylammonium) ethyl methanethiosulfonate (MTSET) from the periplasmic site of the membrane (*23*). Both sites could not be reached by the more bulky charged reagent AmdiS, suggesting a restricted access pathway from the periplasm. In motif mutant S405C, the introduced Cys residue is between Cys398 and Cys414. Treatment of RSO membranes containing S405C with membrane permeable NEM resulted in a rate of inactivation higher than that observed for the wild type with no residual activity, indicating that position 405 is accessible from the water phase (Figure 4C). Remarkably, the transport activity of the S405C mutant was also effectively inhibited by treatment with AmdiS under conditions where the wild type is insensitive to the reagent (Figure 4D). The half-time of inactivation was approximately 4−5 min with essentially no residual activity. Apparently, the Cys residue at position 405 is well exposed to the periplasmic side of the membrane. Mutant S405C was also rapidly inactivated by treatment with the small, positively charged thiol reagent MTSET (not shown). In a control experiment, S405 was replaced with Ala. The S405A mutant was inactivated by NEM at the same rate that was observed for the wild type, and no inactivation was observed with AmdiS (Table 1).

Cysteine-Scanning Mutagenesis of Region Xa of GltS. A set of 17 cysteine mutants of the GltS protein was constructed with mutations in cytoplasmic region Xa between TMS IX and X. Together with Cys343 in wild-type GltS, the mutants cover a stretch of 18 residues from A340 to M357, which represents the most conserved region in the C-terminal half of the ESS family (Figure 1B). Partial purification following expression in *E. coli* DH5α showed that the mutations did not significantly affect the levels of the mutant proteins in the membrane (Figure 5A, top panel). As described above for the Cys mutants in region Vb of

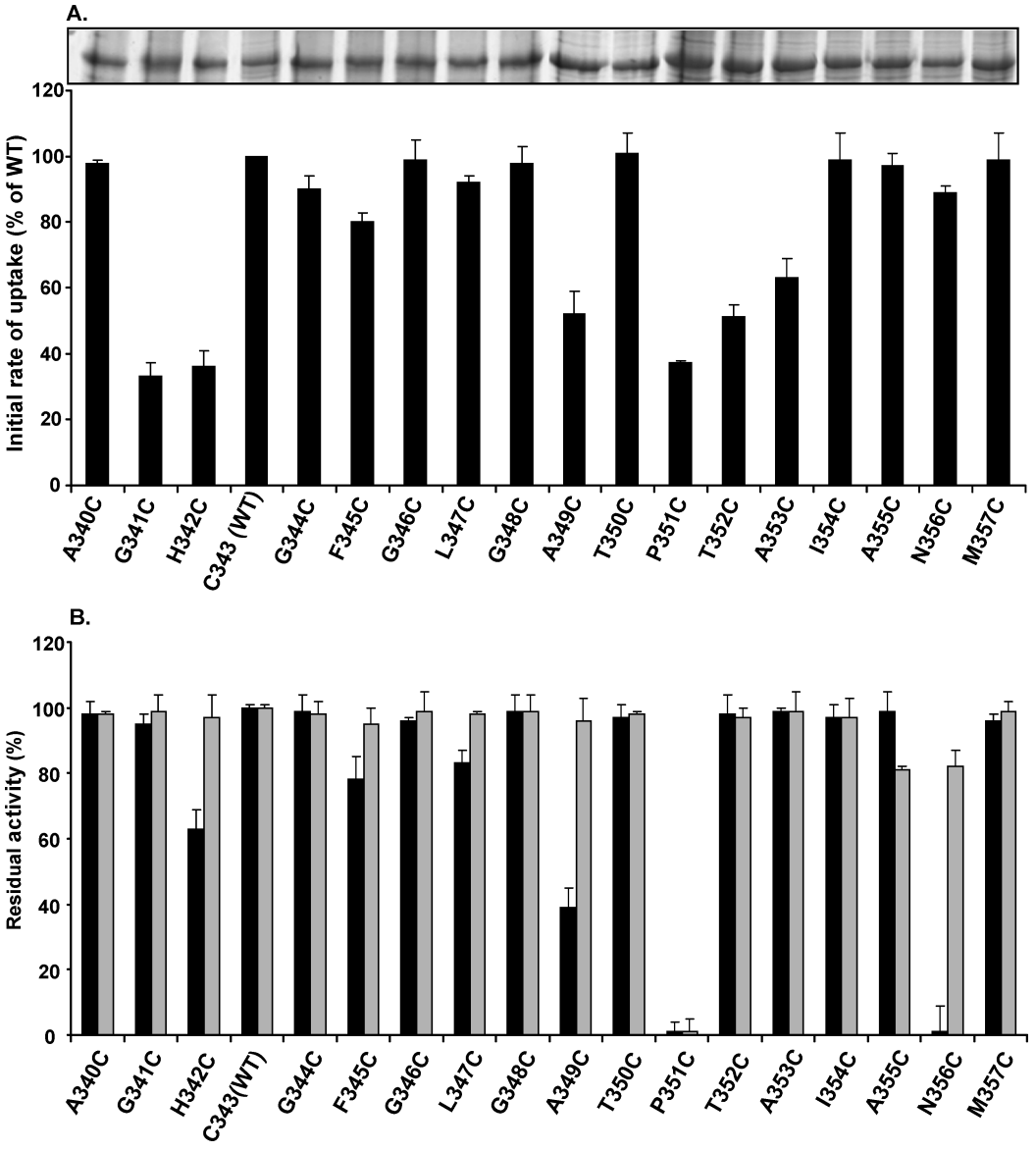

FIGURE 5: Cysteine-scanning mutagenesis of the Xa region of GltS of *E. coli*. (A) Relative L-[^{14}C]glutamate uptake activity in RSO membrane vesicles containing GltS mutants with Cys residues at positions 340−357. Initial rates of glutamate uptake were expressed as a percentage of the rate measured in membrane vesicles containing wild-type GltS (C343). Uptake rates were corrected for the rate observed in control membranes that contained CitS produced from the same expression system (see also Figure 3). Expression levels of wild-type GltS and the mutants after partial purification form cells are indicated at the top. (B) Residual activity of glutamate uptake in RSO membrane vesicles after treatment with 1 mM NEM (black bars) and 0.25 mM AmdiS (gray bars) for 10 min. Residual activity represents the initial rates as a percentage of the initial rate catalyzed by untreated membranes.

GltS, the mutants were tested for their ability to accumulate glutamate in right-side-out (RSO) membrane vesicles (Figure 5A). The mutations were remarkably well tolerated by the transporter. Twelve of the 17 mutants exhibited glutamate uptake activities not significantly different from the wild-type activity. The GltS proteins mutated at the two adjacent positions, G341 and H342, showed a significantly decreased activity that was 30−40% of the wild-type activity. Similarly, a second cluster of four mutants, A349C, P351C, T352C, and A353C, showed an activity that was 30−60% of the wild-type activity.

The wild-type GltS protein contains four cysteine residues, three in transmembrane segments (TMS IV, V, and VI) and one in region Xa at position 343. Nevertheless, it was shown before that the activity of wild-type GltS in RSO membranes is not sensitive to treatment with the membrane permeable thiol reagent NEM or to the membrane impermeable, bulky reagent AmdiS (*10*) (see also Figure 5B, C343). In the group of 12 Xa mutants exhibiting specific activity comparable to that observed for the wild type, only the activity of N356C was dramatically affected by treatment with NEM. The mutant was essentially inactivated by NEM. In contrast, treatment with the membrane impermeable reagent AmdiS did not affect the activity, suggesting that the residue at position 356 is not accessible to the latter in RSO membranes (Figure 5B). In the G341C and H342C pair of mutants that both showed reduced transport activity relative to that of the wild type, the former appeared to be unaffected by both NEM and AmdiS while the latter was marginally sensitive to NEM, resulting in 60% residual activity, and not sensitive to AmdiS. Mutants T352C and A353C in the cluster of four mutants with reduced activity between positions 349 and 353 were also not affected by the thiol reagent, while the activitiy of mutant A349C was reduced to 40% by NEM, but not sensitive to AmdiS. Clearly, the most interesting mutant in this cluster was P351C. P351C was completely inactivated by NEM and, most

Table 2: Residual Activities after Treatment of RSO Membranes Containing GltS Cysteine (Cys) and Alanine (Ala) Mutants in Wild-Type (WT) and Cys-less Background with NEM and AmdiS[a]

		residual activity[b] (%)		
position	inhibitor	Cys/WT	Cys/Cys-less	Ala/WT
P351	NEM	2 ± 4	3 ± 4	100 ± 4
	AmdiS	2 ± 6	4 ± 4	96 ± 2
N356	NEM	1 ± 8	1 ± 5	99 ± 6
	AmdiS	82 ± 5	87 ± 7	96 ± 4

[a] RSO membranes were treated with 1 mM NEM and 0.25 mM AmdiS for 10 min. [b] The indicated values give the residual uptake activity in RSO membranes corrected for the background activity and as the percentage of an untreated sample. The average and standard deviation of two or three independent measurements are reported.

importantly, also by AmdiS. The result indicates that the proline residue at position 351 in cytoplasmic loop Xa of GltS can be accessed from the periplasmic side of the membrane. In this respect, P351 in GltS behaves like residue S405 in region Xa of CitS.

Two types of control experiments demonstrated that the Cys residues at positions 351 and 356 in GltS mutants P351C and N356C, respectively, were the actual target sites for the thiol reagents. One, mutants P351C and N356C in the Cys-less background of GltS (*10*) showed similar residual activities after treatment with NEM and AmdiS as observed in the wild-type background. Two, replacement of P351 and N356 with Ala in the wild-type background rendered the mutant transporters insensitive to treatment by NEM and AmdiS (Table 2).

DISCUSSION

The putative reentrant loop structures in the N- and C-terminal halves of the Na^+-citrate transporter of *K. pneumoniae* CitS and in the N-terminal half of the Na^+-glutamate transporter of *E. coli* GltS contain a GGXG sequence motif. This study demonstrates that these motifs are important for the function of the transporters. Mutant transporters in which the conserved Gly residues of the motifs were replaced with Cys residues were completely inactive or exhibited a severely reduced transport activity. CitS mutants with the variable positions (X) mutated to Cys revealed a lower but significant residual activity, while the corresponding mutant of GltS was inactive. The residual activity appears to correlate with the level of conservation at the X position as the His residue in GltS is, in fact, highly conserved in the family (see sequence logos in Figure 1). Others have shown that mutation of the variable residue in the GGNG motif in the N-terminal half of CitS to Val reduced the affinity for citrate by 1 order of magnitude (*26*). Further evidence for a relevant role of the motifs in the proper functioning of the transporters was obtained by showing that the residual activity of the Cys mutants could be further reduced by treatment with thiol reagents.

Structural models for the CitS and GltS proteins consist of two homologous domains with opposite orientations in the membrane (*11*) (Figure 1A). Prominent in the models are two reentrant loops that fold back between the transmembrane segments from opposite sides of the membrane. These are the regions in the sequence that contain the GGXG motifs. The present results give support to the models in two important aspects: (i) CitS and GltS proteins share a similar fold, and (ii) the proteins have a two-domain structure.

The CitS and GltS proteins belong to different transporter families (2HCT and ESS, respectively) and do not share any sequence similarity. The same structural model for both CitS and GltS is based on the highly similar family hydropathy profiles of the transporters in the 2HCT and ESS families (*2*). In the MemGen classification system, the 2HCT and ESS families are in structural class ST[3] together with 31 other families of transport proteins (*4*) (http://molmic35.biol.rug.nl/memgen/mgweb.dll). The hypothesis is that the proteins from all families in one structural class have the same fold. The membrane topology of the CitS and GltS proteins in the models was recently confirmed experimentally by Cys accessibility studies (*10*). The functional importance of the GGXG motifs in corresponding parts of the CitS and GltS sequences reported here provides further evidence of the similar structure and mechanism of the two transporters.

The two-domain structure in the CitS and GltS models is based on sequence analysis of all protein families in structural class ST[3] in the MemGen classification reported previously (*15*). A low but significant level of sequence identity was identified when the N-terminal halves of the proteins were compared to the C-terminal halves, suggesting sequence homology between the two halves that, consequently, would fold into two domains sharing a similar fold. The putative reentrant loop in the N-terminal domain in the model is a copy of the reentrant loop in the C-terminal domain that has been demonstrated experimentally in the CitS and GltS proteins (see below). Mutation of the three Gly residues to Cys in both GGXG motifs of CitS inactivates or strongly reduces the activity, while mutation of the variable residue reduces the activity to 40−75% in the motifs in the N- and C-terminal halves. The "functional symmetry" strongly supports the "structural symmetry" of the two domains and provides, for the first time, strong experimental support for the reentrant loop structure in the N-terminal domain.

Reentrant loops in membrane proteins are identified by accessibility studies of sites (usually Cys residues) in loop regions. Accessibility of the Cys residue from the opposite side of the membrane by water-soluble, membrane impermeable thiol reagents is taken as evidence that the loop folds between the transmembrane segments exposing the residue more or less to the opposite side of the membrane. In the case of the CitS protein, two endogenous Cys residues, Cys398 and Cys414, in the putative reentrant loop in the C-terminal domain were shown to be accessible for the membrane impermeable thiol reagent MTSET from the periplasmic side of the membrane (*23*). The reactivities of the sites could be modified by the presence of the substrate citrate and the co-ion Na^+, providing further evidence for an important functional role in catalysis. In GltS, two engineered Cys residues at positions 339 and 355 in the putative reentrant loop region in the C-terminal domain were accessible to MTSET from the periplasm as well (*10*). For both transporters, the Cys residues were not accessible for the more bulky reagent AmdiS, suggesting a size restriction in the access pathway from the periplasm which would be compatible with a funnel-like pore structure with the target sites deep down in the narrow part (*24*). The characteristics of the putative reentrant loops in the C-terminal domains of CitS and GltS differed in this respect from those of a reentrant loop in the glutamate transporter GltT of *Bacillus stearothermophilus*. GltT, a glutamate transporter not be confused with GltS, has a completely different structure, but like the CitS/GltS model, two reentrant loops enter the core of the protein from opposite sites of the membrane. The reentrant loops were confirmed by the crystal structure of the homologous transporter Glt_{Ph} of the archaeon *Pyrococcus horikoshi* (*27*).

Accessibility studies of Cys residues engineered in the loop entering from the cytoplasmic side in GltT showed that three consecutive positions were accessible for the bulky AmdiS reagent from the periplasmic side (*28*). The present results now demonstrate that a similar situation exists for the CitS and GltS proteins. Residue S405 at the variable position in the GGXG motif of CitS and P351 of GltS were both accessible for AmdiS added at the periplasmic side of the membrane. This suggests that these positions are closest to the periplasm and at the vertex of the reentrant loop. It was noted before that the putative reentrant loops in the ST[3] structural class contain an unusually high fraction of residues with small side chains which was interpreted as being indicative of a compact packing of the loops between the helices with a strong bending at the vertex allowed by the Gly residues in the GGXG motif (*11*). The accessibility of S405 in the GGXG motif of CitS by AmdiS is in line with the latter view. In GltS, which lacks the GGXG motif in the C-terminal domain, the P351 residue is flanked by Ala and polar Thr residues (ATPTA) which to some extent resembles the vertex of the reentrant loop in GltT of *B. stearothermophilus* which contains a Glu residue flanked by Ala and polar Ser and Thr residues (TASSET). Please note that nine of the 18 residues that form the putative reentrant loop in the C-terminal domain of GltS have small side chains [A, G, or C (Figure 1B)].

By analogy to transporter Glt_{Ph} of the archaeon *P. horikoshi* (*27*), it is believed that the reentrant loops in the N- and C-terminal domains of the ST[3] transporters are in close vicinity in the three-dimensional structure of the proteins where they would form the translocation path for substrates and co-ions (*11*). Turnover would follow an alternating access mechanism by which the translocation pore would open up to either side of the membrane in an alternating manner (*24*). It is easy to envision how changes to the reentrant loops that make up the translocation path could interfere with this process, thereby explaining the high sensitivity of the GGXG motifs to mutations and chemical modifications. Possibly, in the conformational state with the pathway opened up to the cytoplasm, alkylation of the Cys residue at position 356 in GltS mutant N356C which is five positions from P351 at the vertex blocks the cytoplasmic access pathway to the pore, thereby inactivating the transporter (Figure 5B). Also, given the dynamic nature of the protein in the alternate access model, the reactivity of sites on the reentrant loops with thiol reagents may be sensitive to changes in the equilibrium between the inward and outward conformations. Three conditions have been shown to affect the sensitivity of CitS to thiol reagents in a similar way, two mutations, C398S in the Xa region (*23*) and G187A in the Vb region (this study), and the presence of the proton motive force (*23*). The three conditions do not affect the (in)sensitivity of CitS to AmdiS which is diagnostic for the periplasmic access pathway but increase the sensitivity to membrane permeable NEM. Possibly, the Cys residues in the reentrant loop in region Xa (Cys398 and/or Cys414) that are the target sites for the reagents have become more accessible under these conditions by a shift of the equilibrium toward the inward conformation. Clearly, the proximity of the two putative reentrant loops in the three-dimensional structure has to be demonstrated experimentally. Such experiments are in progress.

REFERENCES

1. Saier, M. H.Jr. (2000) A functional-phylogenetic classification system for transmembrane solute transporters. *Microbiol. Mol. Rev. 64*, 354–411.
2. Lolkema, J. S., and Slotboom, D. J. (1998) Estimation of structural similarity of membrane proteins by hydropathy profile alignment. *Mol. Membr. Biol. 15*, 33–42.
3. Lolkema, J. S., and Slotboom, D. J. (1998) Hydropathy profile alignment. A tool to search for structural homologues of membrane proteins. *FEMS Microbiol. Rev. 22*, 305–322.
4. Lolkema, J. S., and Slotboom, D. J. (2003) Classification of 29 families of secondary transport proteins. *J. Mol. Biol. 327*, 901–909.
5. Lolkema, J. S., and Slotboom, D. J. (2005) Sequence and hydropathy profile analysis of two classes of secondary transporters. *Mol. Membr. Biol. 22*, 177–189.
6. Yamashita, A., Singh, S. K., Kawate, T., Jin, Y., and Gouaux, E. (2005) Crystal structure of a bacterial homologue of the Na^+/Cl^--dependent neurotransmitter transporters. *Nature 437*, 215–223.
7. Faham, S., Watanabe, A., Mercado Besserer, G., Cascio, D., Specht, A., Hirayama, B. A., Wright, E. M., and Abramson, J. (2008) The crystal structure of a sodium galactose transporter reveals mechanistic insights into Na^+/sugar symport. *Science 321*, 810–814.
8. Weyand, S., Shimamura, T., Yajima, S., Suzuki, S., Mirza, O., Krusong, K., Carpenter, E. P., Rutherford, N. G., Hadden, J. M., O'Reilly, J., Ma, P., Saidijam, M., Patching, S. G., Hope, R. J., Norbertczak, H. T., Roach, P. C., Iwata, S., Henderson, P. J., and Cameron, A. D. (2008) Structure and molecular mechanism of a nucleobase-cation-symport-1 family transporter. *Science 322*, 708–713.
9. Lolkema, J. S., and Slotboom, D. J. (2008) The major amino acid transporter superfamily has a similar core structure as Na^+-galactose and Na^+-leicine transporters. *Mol. Membr. Biol. 25*, 567–570.
10. Dobrowolski, A., Sobczak-Elbourne, I., and Lolkema, J. (2007) Membrane Topology Prediction by Hydropathy Profile Alignment: Membrane Topology of the Na^+-Glutamate Transporter GltS. *Biochemistry 46*, 2326–2332.
11. Sobczak, I., and Lolkema, J. S. (2005) The 2-hydroxycarboxylate transporter family: Physiology, structure, and mechanism. *Microbiol. Mol. Biol. Rev. 69*, 665–695.
12. Kalman, M., Gentry, D. R., and Cashel, M. (1991) Characterization of the *Escherichia coli* K12 gltS glutamate permease gene. *Mol. Gen. Genet. 225*, 379–386.
13. Deguchi, Y., Yamato, I., and Anraku, Y. (1990) Nucleotide sequence of gltS, the Na^+/glutamate symport carrier gene of *Escherichia coli* B. *J. Biol. Chem. 265*, 21704–21708.
14. Krogh, A., Larsson, B., von Heijne, G., and Sonnhammer, E. L. (2001) Predicting transmembrane protein topology with a hidden Markov model: Application to complete genomes. *J. Mol. Biol. 305*, 567–580.
15. Lolkema, J. S., Sobczak, I., and Slotboom, D. J. (2005) Secondary transporters of the 2HCT family contain two homologous domains with inverted membrane topology and trans re-entrant loops. *FEBS J. 272*, 2334–2344.
16. Lolkema, J. S. (2006) Domain structure and pore-loops in the 2-hydroxycarboxylate transporter family. *J. Mol. Microbiol. Biotechnol. 11*, 318–325.
17. Fu, D., Libson, A., Miercke, L. J., Weitzman, C., Nollert, P., Krucinski, J., and Stroud, R. M. (2000) Structural determinants of water permeation through aquaporin-1. *Science 290*, 481–486.
18. Khademi, S., O'Connell, J.III, Remis, J., Robles-Colmenares, Y., Miercke, L. J. W., and Stroud, R. (2004) Mechanism of ammonia transport by Amt/MEP/Rh: Structure of AmtB at 1.35 Å. *Science 305*, 1587–1594.
19. Van den Berg, B., Clemons, W. M.Jr., Collinson, I., Modis, Y., Hartmann, E., Harrison, S. C., and Rapoport, T. A. (2004) X-ray structure of a protein-conducting channel. *Nature 427*, 24–26.
20. Hunte, C., Screpanti, E., Venturi, M., Rimon, A., Padan, E., and Michel, H. (2005) Structure of a Na^+/H^+ antiporter and insights into mechanism of action and regulation by pH. *Nature 435*, 1197–1202.
21. Kaback, H. R. (1974) Transport in isolated bacterial membrane vesicles. *Methods Enzymol. 31*, 698–709.
22. Konings, W. N., Barnes, E. N.Jr., and Kaback, H. R. (1971) Mechanisms of active transport in isolated membrane vesicles. 2. The coupling of reduced phenazine methosulfate to the concentrative uptake of β-galactosides and amino acids. *J. Biol. Chem. 246*, 5857–5861.
23. Sobczak, I., and Lolkema, J. S. (2003) Accessibility of cysteine residues in a cytoplasmic loop of CitS of *Klebsiella pneumoniae* is controlled by the catalytic state of the transporter. *Biochemistry 42*, 9789–9796.
24. Sobczak, I., and Lolkema, J. S. (2004) Alternating access and a pore-loop structure in the Na^+-citrate transporter CitS of *Klebsiella pneumoniae*. *J. Biol. Chem. 279*, 31113–31120.

25. Deguchi, Y., Yamato, I., and Anraku, Y. (1989) Molecular cloning of gltS and gltP, which encode glutamate carriers of *Escherichia coli* B. *J. Bacteriol. 171*, 1314–1319.
26. Kästner, C. N., Dimroth, P., and Pos, K. M. (2000) The Na^+-dependent citrate carrier of *Klebsiella pneumoniae*: High level expression and site directed mutagenesis of asparagine-185 and glutamate-195. *Arch. Microbiol. 174*, 67–73.
27. Yernool, D., Boudker, O., Jin, Y., and Gouaux, E. (2004) Structure of a glutamate transporter homologue from *Pyrococcus horikoshii*. *Nature 431*, 811–818.
28. Slotboom, D.-J., Sobczak, I., Konings, W. N., and Lolkema, J. S. (1999) A conserved serine-rich stretch in the glutamate transporter family forms a substrate-sensitive re-entrant loop. *Proc. Natl. Acad. Sci. U.S.A. 96*, 14282–14287.